

Diabetic Retinopathy Detection Using Machine Learning and Texture Features

Mohamed Chetoui, Moulay A. Akhloufi, Mustapha Kardouchi
 Perception, Robotics, and Intelligent Machines Research Group (PRIME),
Dept. of Computer Science, Université de Moncton
 Moncton, NB, Canada
 {emc7409, moulay.akhloufi, mustapha.kardouchi}@umanitoba.ca

Abstract—Diabetic retinopathy (DR) is a medical condition due to diabetes mellitus that can damage the patient retina and cause blood leaks. This condition can cause different symptoms from mild vision problems to complete blindness if it is not timely treated. Hemorrhages, hard Exudates, and Micro-aneurysms (HEM) that appear in the retina are the early signs of DR. Early diagnosis of HEM is crucial to prevent blindness. Textures features such as LBP have been widely used in the past as a technique for DR detection. In this work, we introduce the use of different texture features for DR, mainly Local Ternary Pattern (LTP) and Local Energy-based Shape Histogram (LESH). We show that they outperform LBP extracted features. Support Vector Machines (SVM) are used for the classification of the extracted histogram. A histogram binning scheme for features representation is proposed. The experimental results show that LESH is the best performing technique with an obtained accuracy of 0.904 using SVM with a Radial Basis Function kernel (SVM-RBF). Similarly, the analysis of the ROC curve shows that LESH with SVM-RBF gives the best AUC (Area Under Curve) performance with 0.931.

Keywords— Diabetic retinopathy, LESH, LTP, machine learning, SVM.

I. INTRODUCTION

In the last decade, the analysis of internal eye and retinal fundus images has played a key role in human recognition (biometrics), and in acquiring vital information about the health of the human visual system, thus helping in early detection of some pathologies such as glaucoma and diabetic retinopathy [1].

The eye is one of the most important and sensitive part of the human body. The inner part of the eye, facing the lens, includes retina, optic disc, macula, and fovea. It can be seen during an eye exam by looking through the pupil. The retina is sensitive to light. Ophthalmologists examine retinal images manually. These images, known as retinal fundus images, are captured by specialized cameras and are used in medical diagnosis.

Diabetic retinopathy (DR) is a condition where the retina of a diabetic patient is damaged due to blood leaks from retina blood vessels [1-4]. If not timely treated, the patient may suffer from complete blindness. DR progresses without showing any symptoms in its early stages. To avoid serious complications, patients are advised to make regular eye exams. The exudates and micro-aneurysms are the first signs that appear in the retina at the initial stage of DR. The next stage is the appearance of hemorrhages. Early diagnosis of HEM at an early stage is crucial in order to avoid severe complications leading to blindness [1-

4]. Figure 1 shows examples of a normal retina and a DR damaged retina.

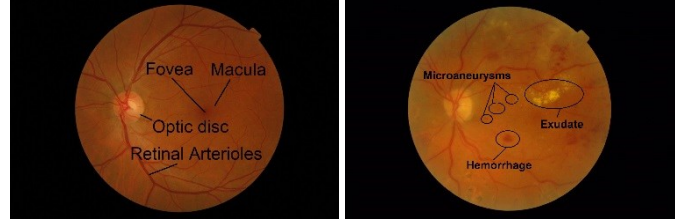


Fig. 1. Example of a normal retina (left) and diabetic retinopathy (right)

Many researchers have devoted their effort to develop an automatic Computer-Aided Detection (CAD) system for DR. Various approaches have been proposed [1-4], but HEM detection in the retinal fundus images and its accuracy are still a big challenge. The limitations are mainly due to the spherical shape of the eye, leading to a brighter region in the center of the retina and dark regions in the borders. Non-uniform lighting, low contrast, small lesions, and the presence of objects in a normal retina that have similar attributes to HEM [1] such as optic disc, blood vessels, etc. make it difficult to accurately identify HEM. HEM is characterized by tiny spots that can be lost during image processing.

Some work has been proposed to detect DR using texture features to preserve the HEM structure. In [2], the authors use Local Binary Patterns (LBP) for the detection of hemorrhages and exudates (HMA). The tests were performed on a database of 89 images. They obtained an average accuracy of 86.15% and an AUC of 0.87. In [3], the authors used fluorescein angiography (FA) fundus images to detect micro-aneurysms (MA). They used Radon transform (RT) and multi-overlapping windows. Tests were conducted on three databases of respectively 120, 50, and 22 images. The authors report the obtained best results for the two first databases with respectively sensitivity and specificity of 94% and 75% for the first database and 100% and 70% for the second one. MA can be easily detected using this imaging modality, but the procedure needs the administration of some injections to the patient, making this approach less interesting as it can cause non-desirable health effects. The best way to examine the retinal fundus is still to use standard retinal fundus imaging technologies. In [4], discrete wavelet transforms are used. The wavelet decomposition was performed up to the second level. Eight energy features were extracted. Two features from the coefficients of two levels and six energy values in three orientations (horizontal, vertical, and diagonal). Classification was performed using Support Vector Machines (SVM) with

different kernels. The authors collected 240 retinal fundus images (120 normal and the remaining with different degrees of DR). They reported a result for accuracy, sensitivity, and specificity of 99% using SVM with polynomial kernel of order 3. The results of these research works are interesting, however the number of images used for experimental tests is small. In recent years, deep learning techniques were proposed for DR detection. Gulshan *et al.* [5] trained an Inception-v3 Convolutional Neural Networks (CNN) using a dataset of 128,175 retinal images, they report an AUC performance of 0.991. Ting *et al.* [6] trained a deep convolutional network in 71,896 retinal images and obtained an AUC of 0.936. They experimented using 10 additional datasets, and obtained an AUC ranging from 0.889 to 0.983. Deep learning techniques are data hungry and need large image numbers for training. In this work we use an available public dataset that has a limited number of images.

Past work dealing with DR using texture features, has mainly focuses on Local Binary Patterns (LBP) [7] and wavelet features. In this work, we propose the use of new texture features to detect DR, mainly Local Ternary Patterns (LTP) [8] and Local Energy-based Shape Histogram (LESH) [9]. The extracted features will be used to build a histogram that can be feed to an SVM classifier [10]. A feature histogram binning is proposed to reduce the number of features to be classified, while still getting high performances. Different kernels are analyzed, and the best performing techniques are presented in the experimental results. The performance of the proposed techniques is evaluated using MESSIDOR dataset [11] containing 1200 images. Average accuracy (ACC) and area under ROC (Receiver Operating Characteristic) curve (AUC) are measured in a k-fold cross-validation scheme.

II. PROPOSED APPROACH AND DATABASE

For the extraction of HEM and the detection of DR, we propose the use of texture features extracted from the retinal fundus images. SVM is used to learn the features characterizing normal images from those showing the presence of DR.

For experimental validation, we used a public database called MESSIDOR [11]. This database contains 1200 color images of the eyes retinal fundus acquired by 3 ophthalmologic departments. They used a 3 CCD camera on a Topcon TRC NW6 non-mydiatic retinograph with a 45 degrees field of view. The captured images have resolutions of 1440*960, 2240*1488 or 2304*1536 pixels and they are encoded using 8-bits per channel. Medical experts provided the diagnosis for each image and evaluated the presence of DR and a retinopathy grade. 540 images were graded as normal, 153 as mild, 247 as moderate, and 260 as severe.

In this work, we want to detect if DR is present or not, only two classes will be considered. The database is labeled as normal for all the images with no DR and as abnormal for all the images with DR, no matter the grade of the retinopathy. In addition, since we are interested in extracting structural features using the retinal image fundus, we convert the color images to grayscale for further processing.

III. FEATURE EXTRACTION

The proposed approach extracts texture features for learning and classification, more specifically: Local Ternary Pattern (LTP) and Local Energy-based Shape Histogram (LESH) described in the following.

A. Local Ternary Pattern (LTP)

Local Ternary pattern texture descriptor was proposed in [8] as an improvement to Local Binary Pattern descriptor [7]. Since LBP is known to be sensitive to noise, LTP uses a fixed threshold to make binary patterns extraction more robust. LTP computation is given by equation 1:

$$LTP_{P,r,\tau} = \sum_{i=0}^{P-1} s(P_i - P_c) \times 3^i, \quad s(x) = \begin{cases} 1 & x \geq \tau \\ 0 & |x| < \tau \\ -1 & x \leq -\tau \end{cases} \quad (1)$$

where τ is a threshold specified by the user, P_c is the central pixel, P_i the neighboring pixel. To reduce the feature dimension, the authors in [8] divide each ternary model into two parts (the positive part and the negative part). Figure 2, shows the results of performing LTP and LBP in a grayscale retinal fundus image.

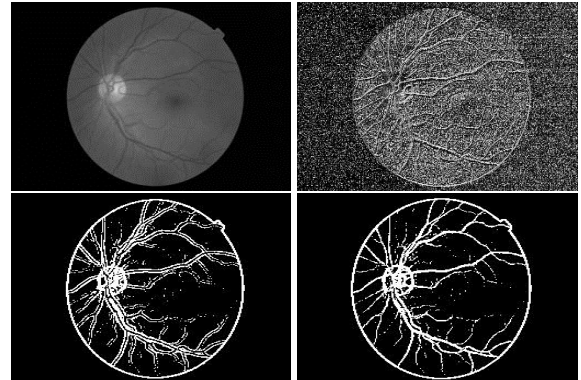


Fig. 2. LTP (from left to right): 1st row: original image, and LBP; 2nd row: LTP lower, and LTP upper

After the image processing using LTP, two feature histograms are obtained for each image (upper and lower). Each histogram is normalized using a bin-width of 25. The results are two vectors of dimension 25 each. In this work, the best performing threshold was equal to 5 [12]. A similar histogram was extracted from the LBP image and can serve as a baseline for comparison with other LBP texture-based DR techniques.

Preliminary results, showed that the LTP upper was performing better than the lower counterpart. In the remaining we will use the upper histogram.

B. Local Energy model and Local Energy-based Shape Histogram (LESH)

The local energy model developed in [13] collects the characteristics at points of an image where the local frequency components are maximized in term of phase. To obtain the phase, the image is convolved with a bank of Gabor filters with 5 spatial frequencies and 8 orientations. At each image location, for each scale and direction, it computes the magnitude and phase of the associated pixel. Originally in [12], the authors proposed to use the cosine of the difference of each phase

component of the average phase as a measure of the phase symmetry. However, this measure is sensitive to noise and results in a poor location. The framework was extended in [14] to use a modified measure consisting of the phase deviation sine, including a weighting factor of the frequency and a noise cancellation factor. The proposed measure is invariant to non-uniform lighting and contrast variation present in the image. This local energy model detects the points of interest in the images with high reliability even in the presence of light variation and noise. In [14], the author proposes the measurement of normalized energy, also called Phase congruency.

The local orientation energy response varies depending on the underlying form such as corners, edges, and boundaries. We compute a local histogram accumulating the local energy along each Gabor filter orientation on different sub-regions of the image. The local histograms are taken from different sub-regions of the image, and then concatenated together. We do this by getting a map orientation label where each pixel is assigned the label of direction where it has the largest energy. The local histogram h is computed using equation 2:

$$h_{r,b} = \sum w_r \times E \times \delta(L - b) \quad (2)$$

Where the subscript b represents the current box, L is the map of orientation label, E is the local energy as proposed in [9], and w is a Gaussian weighting centered on region r . This weight is used to provide soft margins through the bins by allowing small weighted overlap between neighboring sub-regions to overcome scale variation problems. In our experiments, for a 32x32 area, the Gaussian standard deviation σ is set to 20 in both directions.

The resulting feature histogram is a vector of 512 dimensions. Figure 3, shows the results of preprocessing a grayscale retinal fundus image and the resulting Local energy map and orientation map.

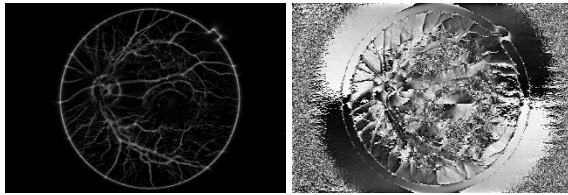


Fig. 3. LESH (image of figure 2) Local Energy map, and Orientation map

IV. CLASSIFICATION

SVM is used for learning and classification of the extracted features. The database is divided into two classes of normal retinal images and DR images.

The feature vectors of LTP and LESH are fed to SVM in order to learn from the extracted vectors the patterns that best represent the retinal fundus images of a normal eye vs an eye showing signs of DR. The learned models can be used later for the classification of the images into DR or Non-DR classes.

Basically, SVM is a linear classifier that extracts the vectors defining the best margin that separate different classes of data. When the data is not linearly separable, kernel tricks are used to define a kernel function that help project feature vectors into a higher dimensional space where they become linearly separable.

Different kernel functions are available such as Radial Basis Functions (RBF), polynomial, etc.

V. EVALUATION METRICS

In medical imaging and diagnosis, detection methods are evaluated using statistical measures such as sensitivity, specificity, accuracy, and Receiver Operating Characteristic curves (ROC) [15]. Accuracy and Area under the ROC curve (AUC) are the most popular and will be used in this work.

The accuracy (ACC) is defined by equation 3 as follows:

$$ACC = (TP + TN) / (TP + TN + FP + FN) \quad (3)$$

Where TP = number of true positives, TN = number of true negatives, FN = number of false negatives, and FP = number of false positives. The accuracy describes the overall rate of the retinal fundus images that were classified correctly.

Another measure used in this work is the Area under the curve (AUC). It is computed as the total area under the ROC curve and measures of how well we can distinguish between two diagnostic classes (abnormal/normal). AUC is particularly useful in the presence of unbalanced data (large number of normal vs disease).

VI. EXPERIMENTAL RESULTS

As mentioned above, the MESSIDOR database images were organized into two classes labeled as 0 (non-DR) and 1 (DR). LTP and LESH descriptors were extracted from the images (figure 4) and used for learning and classification. The data was divided into 10 sets. A 10-fold cross validation was performed on these sets and average results were computed.

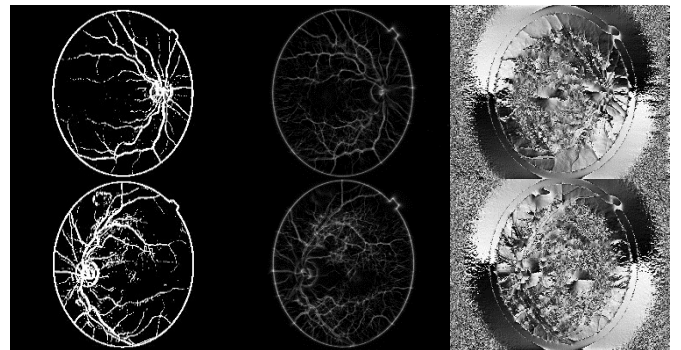


Fig. 4. Example of preprocessed images (from left to right): LTP upper, Local Energy map, and Orientation map

Many tests were conducted to select the best SVM kernels and optimize the hyper-parameters. SVM with RBF was the best performing followed by the polynomial kernel for the LTP accuracy.

Table I gives the ACC (accuracy) and AUC (Area under the ROC curve) results for the different tests. We can see that LTP gives a very interesting performance. However, LESH is the best performing and obtain an ACC of 0.904 using SVM with RBF kernels. The same higher performance is obtained by LESH for AUC with RBF kernels which gives 0.931. These results outperform LTP counterparts and show the robustness of LESH features in classifying DR. In the other hand, we can see that the LBP performance is lower than LTP and LESH.

TABLE I. CLASSIFICATION RESULTS

SVM	ACC			AUC		
	Lin	Poly	RBF	Lin	Poly	RBF
LBP	0.805	0.813	0.823	0.847	0.884	0.897
LTP	0.822	0.869	0.841	0.881	0.914	0.916
LESH	0.865	0.881	0.904	0.904	0.917	0.931

Figure 5 shows the ROC curves used for the computation of AUC for the best obtained performance of each texture analysis technique and for both measures (shown in bold in Table I above). We can clearly see that LESH with SVM-RBF quickly converges to the best results and obtains more true positives for a small number of false positives compared to LTP and LBP. This explains the obtained performance of LESH in term of both ACC and AUC.

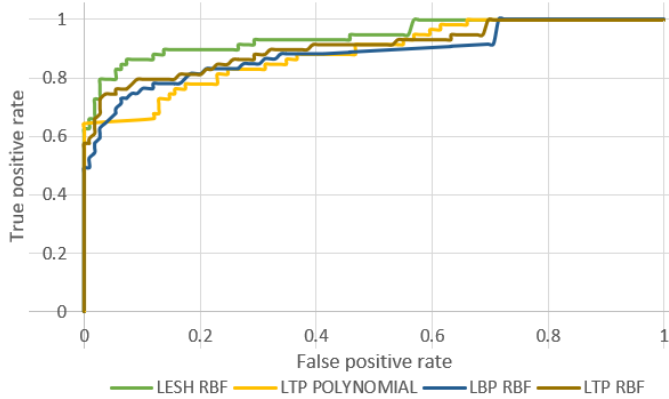


Fig. 5. ROC curve for the best performing LESH, LTP and LBP

VII. CONCLUSION

The increase in diabetes cases limits the ability of current manual testing. New algorithms for assisted diagnosis are becoming very important today. Early detection of diabetes can help the patients and limits the bad health consequences such as blindness. Using retinal fundus images can help automate the diagnosis. Micro hemorrhages and aneurysms, known as HEM, are the early signs of diabetic retinopathy (DR) and are difficult to identify because of their similarities with normal parts of a healthy human. Other problems such as non-uniform lighting, low contrast, etc. can lead to a bad diagnosis. Texture based techniques for DR detection were proposed in the past. Most of these techniques use LBP and wavelets for feature extraction from retinal images. In this work, we propose the use of new texture features, mainly LTP and LESH. These techniques capture the local relationship between neighboring pixels and features and are less sensitive to variation in illumination, color, noise, etc. These features extracted from the retinal fundus images are used to learn signs of HEM and differentiate between DR and non-DR. SVM is used to classify these features. Polynomial and RBF kernels were the best performing in the detection of DR. Experimental tests with the MESSIDOR database show that LESH and LTP perform well in detecting DR. Overall, LESH was the best performing with an accuracy of 0.904 and an AUC of 0.931 using SVM with RBF kernels.

The proposed approach is suitable even for small datasets. New techniques based on deep learning are data hungry but show impressive performances in different classification tasks including DR. Future work includes benchmarking the performance of deep learning techniques and the proposed texture-based features in a small dataset such as MESSIDOR.

REFERENCES

- [1] S. Mohammadian, A. Karsaz and Y. M. Roshan, "A comparative analysis of classification algorithms in diabetic retinopathy screening," *2017 7th International Conference on Computer and Knowledge Engineering (ICKE)*, Mashhad, pp. 84-89, 2017.
- [2] M. N. Ashraf, Z. Habib and M. Hussain, "Texture Feature Analysis of Digital Fundus Images for Early Detection of Diabetic Retinopathy," *2014 11th International Conference on Computer Graphics, Imaging and Visualization*, Singapore, pp. 57-62, 2014.
- [3] M. Tavakoli, R. Shahri, H. Pourreza, A. Mehdizadeh, T. Banaee and M. Bahreini Toosi, "A complementary method for automated detection of microaneurysms in fluorescein angiography fundus images to assess diabetic retinopathy," *Pattern Recognition*, vol. 46, no. 10, pp. 2740-2753, 2013.
- [4] K. Noronha, U. R. Acharya, K. P. Nayak, S. Kamath, and S. V. Bhandary, "Decision support system for diabetic retinopathy using discrete wavelet transform," *Proc Inst Mech Eng H*, vol. 227, no. 3, pp. 251–261, 2013.
- [5] V. Gulshan, L. Peng, M. Coram, M. Stumpe, D. Wu, A. Narayanaswamy, S. Venugopalan, K. Widner, T. Madams, J. Cuadros, R. Kim, R. Raman, P. Nelson, J. Mega and D. Webster, "Development and Validation of a Deep Learning Algorithm for Detection of Diabetic Retinopathy in Retinal Fundus Photographs," *JAMA*, vol. 316, no. 22, pp. 2402–2410, 2016.
- [6] D. Ting, C. Cheung, G. Lim, G. Tan, N. Quang, A. Gan, H. Hamzah, R. Garcia-Franco, I. San Yeo, S. Lee, E. Wong, C. Sabanayagam, M. Baskaran, F. Ibrahim, N. Tan, E. Finkelstein, E. Lamoureux, I. Wong, N. Bressler, S. Sivaprasad, R. Varma, J. Jonas, M. He, C. Cheng, G. Cheung, T. Aung, W. Hsu, M. Lee and T. Wong, "Development and Validation of a Deep Learning System for Diabetic Retinopathy and Related Eye Diseases Using Retinal Images From Multiethnic Populations With Diabetes," *JAMA*, vol. 318, no. 22, pp. 2211–2223, 2017.
- [7] T. Ojala, M. Pietikäinen, and D. Harwood, "A comparative study of texture measures with classification based on featured distributions," *Pattern Recognition*, vol. 29, no. 1, pp. 51–59, 1996.
- [8] X. Tan and B. Triggs, "Enhanced Local Texture Feature Sets for Face Recognition Under Difficult Lighting Conditions," in *IEEE Transactions on Image Processing*, vol. 19, no. 6, pp. 1635-1650, 2010.
- [9] S. K. Wajid and A. Hussain, "Local energy-based shape histogram feature extraction technique for breast cancer diagnosis," *Expert Systems with Applications*, vol. 42, no. 20, pp. 6990–6999, 2015.
- [10] A. Ben-Hur, C. S. Ong, S. Sonnenburg, B. Schölkopf, and G. Rätsch, "Support Vector Machines and Kernels for Computational Biology," *PLOS Computational Biology*, vol. 4, no. 10, p. e1000173, 2008.
- [11] E. Decencière, X. Zhang, G. Cazuguel, B. Lay, B. Cochener, C. Trone, P. Gain, R. Ordóñez, P. Massin, A. Erginay, B. Charton, and J-C. Klein, "Feedback on a publicly distributed database: the Messidor database," *Image Analysis & Stereology*, v. 33, n. 3, p. 231-234, 2014.
- [12] A.M. Owen, J.L. Iddon, J.R. Hodges, B.A. Summers, T.W. Robbins, "Spatial and non-spatial working memory at different stages of Parkinson's disease," *Neuropsychologia*, Volume 35, Issue 4, pp. 519-532, 1997.
- [13] R. Owens, S. Venkatesh, and J. Ross, "Edge detection is a projection," *Pattern Recognition Letters*, vol. 9, no. 4, pp. 233–244, 1989.
- [14] P. Kovesi, "Phase Congruency Detects Corners and Edges," *Proc. VIIth Digital Image Computing: Techniques and Applications*, Sydney, Australia, pp309-318, 2003.
- [15] J. A. Hanley and B. J. McNeil, 'The meaning and use of the area under a receiver operating characteristic (ROC) curve', *Radiology*, vol. 143, no. 1, pp. 29–36, 1982.